

RS CVn VERSUS ALGOL-TYPE BINARIES: A COMPARATIVE STUDY OF THEIR X-RAY EMISSION

K. P. SINGH,¹ S. A. DRAKE,² AND N. E. WHITE

Code 660.2, Laboratory for High Energy Astrophysics, NASA/GSFC, Greenbelt, Maryland 20771

Electronic mail: kps@tivrax.tifr.res.in, drake@lheavx.gsfc.nasa.gov, white@adhoc.gsfc.nasa.gov

Received 1995 November 6; revised 1996 February 29

ABSTRACT

We have compiled a list of 59 RS CVn binaries and 29 Algol-type binaries with well-known orbital parameters and which have been observed with the *ROSAT* PSPC detector in order to find out whether there is any detectable influence of mass transfer on the x-ray emission properties of these two types of active binaries. If there were, one might expect the RS CVn binaries (which typically are expected to have negligible mass exchange) and the semidetached “Algol” binaries (which have well-established mass exchange between the two components) to exhibit systematic differences in the x-ray region. We have studied the statistical correlations between (a) the x-ray luminosity (L_x) and the Roche-lobe filling fraction (Γ_2) for the active star, (b) L_x and the rotation period (P), and (c) the x-ray surface flux (S_x) and P . In general, we find that the RS CVn and Algol binaries do not have similar L_x distributions. There is a tendency for the Algol binaries to be ~ 3 – 4 times less luminous compared to RS CVns with the same period. This is the exact opposite of what might have been expected if mass transfer rates influenced x-ray emission levels, since in that case the Algol binaries would be more x-ray luminous than the RS CVn binaries. A highly significant correlation is found between $\log S_x$ and $\log P$ in both of the two types of binaries, while a weak correlation that is observed between $\log L_x$ and $\log \Gamma_2$ in the RS CVn binaries is likely to be due to correlations of these quantities with the stellar radii. © 1996 American Astronomical Society.

1. INTRODUCTION

A wide variety of close binary stars containing at least one late-type component show enhanced activity as compared to single late-type stars of the same spectral and luminosity class. This activity manifests itself in terms of intense Ca II H and K emission, x-ray and radio emission, significant surface area coverage by star-spots, ultraviolet and infrared excesses, and high frequency and magnitude of flaring. Among the most commonly known types of active stars are the RS CVn binary stars which typically can have x-ray luminosities L_x that are 1,000–10,000 times higher than that of the quiet Sun. Apart from the “classical” RS CVn binaries, originally defined by Hall (1976), there are several other classes of binaries containing at least one late-type star which can attain similarly high levels of activity (e.g., see Hall 1989). These include short-period and long-period RS CVn binaries, close binary systems containing a white dwarf or subdwarf secondary, semi-detached (Algol) or detached binaries containing a late-type subgiant as the secondary star and an early-type companion as the primary star, and contact (W UMa-type) binaries.

As pointed out by Hall (1989), Algol-type binaries, most of which are semidetached systems and have mass exchange taking place from the Roche-lobe filling secondary to the

primary star, share almost all the characteristics of activity with the RS CVn binary stars. Conversely, some of the RS CVn stars are also known to be semidetached and thus can also be classified as Algol binaries, e.g., AD Cap, RZ Cnc, RT Lac, RV Lib, and AR Mon, so that these two classes of binaries are not mutually exclusive. However, unlike in the Algol-type binaries where, in general, only one of the component stars is of late spectral type, in RS CVn systems both components are usually late-type and frequently both stars are “active”. As a general rule, in this paper we will use the term “Algol binaries” in its broadest sense so as to include both confirmed semi-detached systems as well as eclipsing binary systems having EA- and EB-type light curves, late B to early F spectral type primaries, and secondaries of similar or later spectral types. [As discussed below, the Roche-lobe filling fraction Γ is the quantitative measure of the binary configuration: true semi-detached binary systems (the rigorous Algols) should have $\Gamma \approx 1$ for one component, while detached systems should have $\Gamma \ll 1$.] From an astrophysical standpoint, the Algols are typically more massive systems than the RS CVn’s, with total masses ranging from ~ 2 – $10 M_\odot$ for the former compared to ~ 2 – $5 M_\odot$ for the latter. In most of the RS CVn systems the more evolved star has a present mass that is similar to or higher than that of the other component, indicating that the evolution of these stars has not been appreciably affected by their binary environment, whereas this is not the case for typical Algol systems, in which the more evolved star is presently of lower mass

¹NRC-NASA Senior Research Associate, on leave from Tata Institute of Fundamental Research, Bombay, India.

²Also Universities Space Research Association.

than its companion, indicating that significant mass-transfer is or has occurred.

The strong x-ray emission of active binary stars is generally attributed to thermal emission from the hot ($\approx 10^6 - 10^{7.5}$ K) coronae of these stars. The rapid rotation of the late-type component(s) in these close binary systems induced by tidal spin-orbit coupling is generally believed to power a rotational-convective dynamo that is responsible for the increased activity in these binary stars. However, it has also been suggested that in some of the detached RS CVn systems there may be ongoing mass transfer which may be responsible for their excess H α luminosities and perhaps also for a good fraction of their x-ray emission (Welty *et al.* 1992; Welty & Ramsey 1995). If this latter hypothesis were correct, one might expect that there should be a correlation of these activity indicators with the mass transfer rate, or some proxy for it such as the Roche-lobe filling fraction Γ of the mass losing star; furthermore, one would predict that semidetached Algol binaries with their better developed degree of mass transfer should exhibit correspondingly higher levels of activity than otherwise similar binary systems that are detached. In fact, Welty & Ramsey (1995) have presented some evidence that L_x and Γ are correlated in a sample of RS CVn binary stars which they have assembled, thus giving some support for this hypothesis. They did not, however, include in their analysis a significant number of Algol binaries, so that the validity of the mass transfer-activity hypothesis for this class of binaries was unclear.

Our motivation in the present paper is to study the x-ray emission properties of active binary stars including significant numbers of both detached and semidetached systems and to determine whether there are any systematic differences between them. We have assembled a set of 59 x-ray observed RS CVn systems with well-known orbital parameters comprising (a) the sample of RS CVn stars studied by Welty & Ramsey (1995), (b) additional x-ray observations of RS CVns that we made with the *ROSAT* PSPC instrument, and (c) further x-ray data on RS CVns that we have selected from the *ROSAT* point source catalog known as WGACAT that is based on the public *ROSAT* archives (White *et al.* 1994). Secondly, we have assembled a set of 29 x-ray observed Algol binaries which comprises all of the eclipsing binary stars of "EA" type which (a) have an early type (mostly B & A types) primary, (b) have binary parameters available from Branczewicz & Dworak (1980), and (c) have been associated with x-ray sources in the WGACAT. As already noted, this second category of binaries will henceforth be referred to as Algol-type binaries even though a number of these binaries are detached rather than semidetached, as indicated by their Γ values.

The details of the sample of RS CVns used by Welty & Ramsey (1995) are given in Sec. 2, along with that of the additional RS CVns from the WGACAT, and those of the active binaries with early-type primaries in the WGACAT are given in Sec. 3. In Sec. 4, we describe the x-ray properties of these systems and examine their correlation with the Roche-lobe filling factors, orbital periods, etc., while in Sec. 5, we discuss the results and present our conclusions.

2. RS CVn BINARIES FROM PUBLISHED *ROSAT* ALL SKY SURVEY AND POINTINGS

We initially adopted the same sample of RS CVn binaries with known binary parameters, distances, and with x-ray detections from the RASS, that was used by Welty & Ramsey (1995). These stars are listed in Table 1(a). In addition, we searched the WGACAT for RS CVn binaries that were detected in deeper pointed observations with the *ROSAT* PSPC and identified seven additional systems (including FF Aqr and HR 9024 that were observed by us). These additional stars are listed in Table 1(b). As in Welty & Ramsey (1995), two of the objects in Table 1(a) have their x-ray luminosities based on observations with the *Einstein*. We dropped EI Eri from our list because of the problems with its orbital parameters which lead to a very high value of Roche-lobe filling fraction (see below), as was pointed out by Welty & Ramsey (1995). In Tables 1(a) and 1(b), we provide the rotational periods, P , and distances, as given in the second edition of the catalog of chromospherically active binary stars (Strassmeier *et al.* 1993, henceforth referred to as CABS2). Using these and the other relevant data given in CABS2, we recalculate the Roche-lobe filling fractions for the stars in each binary system using an approximation formula for the Roche-lobe radius given by Eggleton (1983) viz., $R_L/a = 0.49q^{2/3}/[0.6q^{2/3} + \ln(1 + q^{1/3})]$, where q is the mass ratio of the two stars, and a is their orbital separation. The Roche-lobe filling fraction, Γ_2 , i.e., the ratio of the stellar radius to the Roche-lobe radius, was calculated for the "active" star in the RS CVn binary, wherever this is known (e.g., as indicated in Drake *et al.* 1989); for the remainder, the cooler star was assumed to be the more active one. The spectral types of the assumed active stars are listed in Tables 1(a) and 1(b).

Based on our previous analysis (Singh *et al.* 1995a, Singh *et al.* 1996) and some more recent analysis of the PSPC data (Singh *et al.* 1995b), we adopt a value of 0.94×10^{-11} ergs $^{-1}$ s $^{-1}$, which corresponds to pulse-height channels 24–200 used in the WGACAT for converting the PSPC count rates observed in the WGACAT and the *ROSAT* All Sky Survey (RASS) (see below). The uncertainty due to the difference in the channels used in the WGACAT and RASS is less than $\sim 10\%$. Since the count rate to flux conversion derived by us is about 50% higher than the value used by Dempsey *et al.* (1993a) and retained by Welty & Ramsey (1995), we have recalculated the luminosities for all the stars in Tables 1(a) and 1(b). The higher conversion factor is due to the difference in the elemental abundances in the plasma models used for spectral analyses. The x-ray surface fluxes, S_x , for the stars were also derived assuming that the x-ray luminosities are mostly from the surface of the active star, thus $S_x = L_x/4\pi R_a^2$, where R_a is the radius of the active star in the binary.

3. ALGOL-TYPE BINARIES FROM *ROSAT* POINTINGS

We cross-correlated all the eclipsing binaries with known orbital parameters and early-type (spectral type B or A) or a "hot" companion from the compilations of Giuricin *et al.*

TABLE 1. (a) Properties of selected RS CVn type binaries in RASS.

Name	Spectral ^a Type	Period ^b days	Distance ^b pc	Γ_2^c	PSPC ^d Counts s ⁻¹	L_x^e 10 ³⁰ ergs s ⁻¹	S_x 10 ⁷ ergs cm ⁻² s ⁻¹
ζ And	K1 III	17.7692*	31	0.63	2.08	2.25	0.02
CF Tuc	K4 IV	2.798	54	0.82	1.01	3.3	0.50
UV Pac	K0-2 V	0.86105*	125	0.49	0.95	16.7	33.1
BI Cet ^e	G5 V	0.52006	60	0.72	1.5	6.12	12.4
AR Psc	K2 V	12.245	17	0.12	4.35	1.4	1.0
TZ Tri A	K0 III	14.7339	75	0.79	0.99	6.3	0.06
LX Per	K0 IV	7.905	130	0.33	0.74	14.2	2.5
UX Ari	K0 IV	6.43791	50	0.67	6.57	18.5	1.4
V711 Tau	K1 IV	2.841	36	0.91	24.26	35.4	3.8
V837 Tau ^e	G2 V	1.89	55	0.34	4.3	14.7	24.1
RZ Eri	K0 IV	31.4	143	0.26	0.16	3.7	0.1
α Aur	G1 III	8	13	0.20	25.2	4.8	0.05
CQ Aur	K1 IV	10.56	220	0.74	0.04	2.2	0.05
SV Cam ^e	G2-3 V	0.59307	74	0.71	0.41	2.5	3.4
VV Mon	K0 IV	6.05056	380	0.82	0.14	22.8	1.0
SS Cam	K0 IV -III	4.823	255	0.92	0.07	5.1	0.2
AR Mon	K2-3 III	21.20812*	525	1.04	0.12	37.3	0.3
AE Lyn	G5 IV	10.163	38	0.23	1.40	2.3	0.5
RU Cnc	K1 IV	10.135	300	0.46	0.17	17.2	1.2
RZ Cnc	K3-4 III	21.64303	395	1.00	0.10	17.5	0.2
TY Pyx	G5 IV	3.32	55	0.18	1.91	6.5	3.8
WY Cnc	M2	0:82937	160	0.53	< 0.01	< 0.3	< 1.2
93 Leo	G5 IV-III	55.0	36	0.14	1.17	1.7	0.08
DK Dra ^e	K1 III	63.75	130	0.33	1.69	32.1	0.3
IL Com ^e	F8 V	0.82	86	0.60	0.81	6.7	9.1
UX Com	K1 IV	3.64239	350	0.51	0.19	26.2	6.9

Name	Spectral ^a Type	Period ^b days	Distance ^b pc	Γ_2^c	PSPC ^d Counts s ⁻¹	L_x^e 10 ³⁰ ergs s ⁻¹	S_x 10 ⁷ ergs cm ⁻² s ⁻¹
RS CVn	G9 IV	4.7912	180	0.56	0.80	29.2	3.0
BL CVn	K0 III	18.6917	300	0.95	0.07	7.1	0.05
BH CVn	K2 IV	2.61321*	53	0.84	2.71	8.6	1.7
RV Lib	K3 IV	10.72216	270	0.96	-	11.5	0.4
SS Boo	K0 IV	7.60613	220	0.40	0.06	3.3	0.5
TZ CrB ^e	F6 V	1.1687	21	0.52	10.34	5.1	5.7
WW Dra	K0 IV	4.62962	180	0.63	0.57	20.8	2.2
ε UMi	G5 III	39.4809*	71	0.28	1.45	8.2	0.09
V792 Her	K0 III	27.07	310	0.59	0.34	36.8	0.4
V824 Ara	K0 V-IV	1.682	39	0.33	5.59	9.6	17.0
V965 Sco	K1 III	30.9597	400	0.59	0.19	34.3	0.3
Z Her	K0 IV	3.962	100	0.51	0.37	4.2	0.9
MM Her	K0 IV	7.936	190	0.33	0.14	5.7	1.2
PW Her	K0 IV	2.881	285	0.85	0.15	13.7	1.6
AW Her	G8 IV	8.80076*	315	0.35	0.16	17.8	2.9
V1817 Cyg	K2 III-II	108.854	302	0.77	0.15	15.4	0.007
V1764 Cyg	K1 III	39.878	390	1.52	0.07	12.0	0.04
CG Cyg ^e	G9.5 V	0.631143	63	0.74	0.11	0.5	1.0
ER Vul ^e	G0 V	0.6942	46	0.66	2.89	6.9	9.9
HR 8170	K5 V	3.243347*	29	0.17	0.87	0.8	2.5
AD Cap	G5	2.96	250	1.09	-	25.0	3.8
RT Lac	G9 IV	5.074015	205	0.98	0.14	6.6	0.5
AR Lac	K0 IV	1.98322	47	0.90	7.72	19.2	3.3
RT And	K0 V	0.62893	95	0.58	0.20	2.0	4.7
SZ Psc	K1 IV	3.955	125	0.82	2.44	42.9	2.7
KT Peg	K6 V	6.092	25	0.13	0.35	0.25	0.8

^a Spectral type for the assumed active star.^b Rotation period from Strassmeier et al. (1993). Orbital period assumed for starred entries.^c Roche-Lobe filling fraction calculated following Eggleton (1983) using the stellar data from Strassmeier et al. (1993), except that the RT Lac data are from Popper (1991).^d From Dempsey et al. (1993a; 1993b)^e Count rate to flux conversion factor is 9.4×10^{-12} ergs cm⁻² s⁻¹ count⁻¹

(Data for RV Lib & AD Cap are from Einstein Observations).

(1983), and Brancewicz & Dworak (1980) with the WGACAT. This resulted in 23 Algol-type stellar binary systems having been detected in the *ROSAT* pointings. Five of the classical Algol-type semidetached binaries viz., RZ Cas, U Cep, TW Dra, δ Lib, and β Per, were observed by us and details of their observations and spectral analysis have been reported by Singh *et al.* (1995a). Notice that not all of these 23 systems are actually semidetached, however, and three of the objects in Table 2 are detached systems with β Lyr-type light curve shapes, one of which has an F type primary. The complete set of x-ray detected Algol-type binaries are listed in Table 2 along with their binary types (detached or semidetached), spectral types, orbital periods (which are presumed to be identical to the rotation periods of the active cool components), distances, Roche-lobe filling fractions (Γ_2) of the active stars (as given in Brancewicz & Dworak 1980), count rates in the *ROSAT* PSPC, x-ray luminosities L_x , and x-ray surface fluxes S_x . The x-ray surface fluxes were derived as before, i.e., assuming that all the luminosity arises from the “cool” companions, which should be a perfectly valid as-

sumption as single late B- and A-type main sequence stars

TABLE 1. (b) Properties of additional RS CVn type binaries selected from WGACAT.

Name	Spectral ^a Type	Period ^b days	Distance ^b pc	Γ_2^c	PSPC ^d Counts s ⁻¹	L_x^e 10 ³⁰ ergs s ⁻¹	S_x 10 ⁷ ergs cm ⁻² s ⁻¹
XY UMa ^e	G3 V	0.47899	100	0.85	0.3	3.37	5.76
LR Hya	K0 V	3.1448	34	0.12	0.064	0.08	0.20
BD+25 2511	G9 V	3.5583*	55	0.27	0.24	0.82	1.11
V772 Her	G0 V	0.878	41.7	0.34	1.89	3.7	16.9
FF Aqr	G8 IV-III	9.20775	300	0.41	0.338	34.2	1.50
HR 9024	G1 IIIe	23.25	175	-	0.99	43.0	0.38
IX Per	F5 V	1.326	48	-	0.31	0.83	0.61

^a Spectral type for the assumed active star.^b Rotation period from Strassmeier et al. (1993). Orbital period assumed for starred entries.^c Roche-Lobe filling fraction following Eggleton (1983) & data from Strassmeier et al. (1993)^d From WGACAT (1994)(FF Aqr data from present observations).^e Count rate to flux conversion factor is 9.4×10^{-12} ergs cm⁻² s⁻¹ count⁻¹

TABLE 2. Properties of Algol-type binaries selected from WGACAT.

Name	Type ^a	Spectral Components	Period days	Distance pc	Γ_2	PSPC ^b	L_x^c	S_x
						Counts s ⁻¹	10 ³⁰ ergs s ⁻¹	10 ⁷ ergs cm ⁻² s ⁻¹
DS And	BD	F3+	1.0105	416.7	0.65	0.008	1.5	1.1
R Ara	D	B9+	4.4251	166.7	0.46	0.175	5.4	1.0
AR Aur	D	B9V+B9V	4.1347	135.1	0.27	0.006	0.1	0.05
AW Cam	D	A0+K3	0.7713	344.8	0.66	0.013	1.8	2.15
RZ Cas	S	A2.8V+G1IV	1.1952	78.1	0.97	1.68	11.5	5.6
DO Cas	BD	A2II+K0IV	0.6847	227.3	0.69	0.013	0.8	1.2
SS Cen	S	B9+G8IV	2.4787	500	1.01	0.023	6.5	0.8
U Cep	S	B7V+G8III-IV	2.4931	208.3	0.98	0.381	18.6	1.5
U CrB	D	B6+F2IV	3.4522	500	0.87	0.059	16.4	0.96
α CrB	D	AOV+G3	17.3599	26.3	0.07	0.05	0.04	0.08
Z Dra	S	A5+K3IV	1.3574	555.5	0.95	0.023	7.8	4.8
TW Dra	S	A5V+K0III	2.8068	250.0	1.03	0.113	7.9	0.8
AI Dra	D	A0V+F9	1.1988	238.1	0.89	0.121	7.7	2.4
TT Hya	D	A3+G7IV	6.9534	185.2	0.76	0.017	0.7	0.05
δ Lib	S	A0IV-V+G2III	2.3273	83.3	0.96	0.636	5.0	0.7
V846 Oph	D	A2+	3.12676	580.2	0.40	0.016	6.0	2.1
V1010 Oph	BD	A7V+F8	0.6614	74.1	0.49	0.399	2.5	5.7
DF Peg	D	A2+	14.26	434.8	0.22	0.133	28.3	4.7
β Per	S	B7.7V+G8III	2.8673	27.8	0.98	8.5	7.4	0.94
BS Sct	D	A0III+	3.8210	1000	0.58	0.006	6.9	0.9
V Tuc	D	A2+M0	0.8709	714.3	0.88	0.005	2.6	1.5
TX UMa	S	B8+F7IV	3.0632	256.4	0.97	0.094	7.0	0.4
BE Vul	D	A4V+	1.5520	312.5	0.83	0.007	0.8	0.24
3 σ Upper Limits from PSPC Public Database								
IM Aur	D	B9+K3IV	1.2473	434.8	0.81	0.03	6.3	2.25
S Cnc	D	B9V+G8IV	9.4853	476.2	0.62	0.023	5.9	0.18
DI Peg	S	F4IV+K3	0.71181	200	0.96	0.017	0.7	0.59
XZ Sgr	D	A3V+G5IV	3.27549	263.2	0.89	0.023	1.8	0.55
λ Tau	D	B3.3V+A4IV	3.95295	111.1	0.79	0.003	0.04	0.0035
RS Vul	D	B5+G2IV	4.47766	344.8	0.94	0.02	2.5	0.133

^a D: Detached system, S: Semi-detached system, BD: β Lyr Detached system

^b From WGACAT Rev 1.0 using PH channels 24 – 200

^c Using conversion factor of 9.4×10^{-12} ergs cm⁻² s⁻¹ count⁻¹ (see text)

Note: Optical data are from Brancewicz & Dworak (1980)

rarely (if ever) emit x-rays. In addition, we searched the publicly available *ROSAT* PSPC database for observations of Algol-type binaries nearer than 500 pc listed by Giuricin *et al.* (1983) and Brancewicz & Dworak (1980), and obtained upper limits on L_x for six additional Algol-type systems. These are listed separately in Table 2.

4. X-RAY PROPERTIES OF ACTIVE BINARIES

In Fig. 1, we have plotted histograms of the distribution of x-ray luminosity (L_x) of all the active binary stars in Tables 1 and 2. The effect of upper limits for some of the Algols is shown separately in Fig. 1. It is important to note here that the samples of RS CVns and Algols are not statistically complete. A cursory glance at Fig. 1 shows the two histograms for the RS CVns and Algols to be quite similar. A closer examination, however, reveals significant differences. For example, the number of high L_x objects in the RS CVn and Algol samples in Fig. 1 and Table 3 are very different—there are 12 RS CVns (20% of the RS CVn sample) with $L_x > 21 \times 10^{30}$ ergs s⁻¹ compared to only 1 Algol system (<4% of the Algol sample). To further examine the two distributions and test the significance of the differences, we

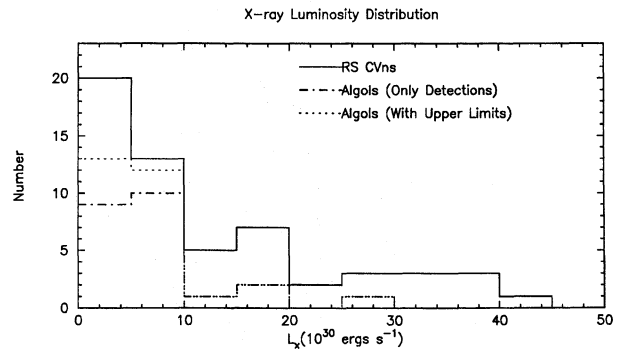


FIG. 1. Histogram of L_x for the sample of RS CVns, and Algol-type stellar binaries.

used the Kaplan Meier estimator and carried out two-sample statistical tests in the ‘‘ASURV’’ set of programs (Isobe *et al.* 1986) in the IRAF/STSDAS software package. The cumulative x-ray luminosity functions derived from the Kaplan Meier estimator are shown in Fig. 2. The distributions are not only different at the high L_x end, but even the median and the mean values of the two distributions are found to be significantly different. The median value of L_x is 6.8×10^{30} ergs s⁻¹ for RS CVns, and 2.8×10^{30} ergs s⁻¹ for Algols. The results from the various types of two-sample tests are listed in Table 3. A consistently low value of probability ($P \leq 0.006$) for the set based on all the available two-sample tests, except the Peto Prentice Wilcoxon test, shows that the two samples of RS CVns and Algols are not from the same population, confirming the results based on the Kaplan Meier estimator. The difference in the two samples, however, tends to vanish as the higher luminosity objects from the sample are excluded from the tests. To summarize, the Algol-type binaries are generally subluminous by a factor ~ 3 as compared to the RS CVn binaries and, in particular, there is a lack of high L_x objects among the Algols.

We have studied the correlation between various parameters of the active binaries in our sample using the statistical tests in the ‘‘ASURV’’ set of programs (Isobe *et al.* 1986). In particular, we calculated the generalized Kendall’s τ correlation coefficient, Spearman’s rank order ρ , and the intercept and slope for the correlation using the Buckley–James

TABLE 3. Results of two-sample tests.

Sample and Number of Objects in Two Groups			
$L_x (\times 10^{30} \text{ ergs s}^{-1})$ Range	≤ 50	≤ 21	≤ 15
Number of RS CVns	59	47	39
Number of Algols	29	28	26
Probability of having a common parent L_x distribution			
Gehan’s Generalized Wilcoxon Test	0.0045	0.0593	0.1556
(Permutation Variance)			
Gehan’s Generalized Wilcoxon Test	0.0061	0.0638	0.1595
(Hypergeometric Variance)			
Logrank Test	0.0031	0.0198	0.0431
Peto and Peto Generalized Wilcoxon Test	0.0040	0.0533	0.1394
Peto and Prentice Generalized Wilcoxon Test	0.0330	0.2499	0.5168

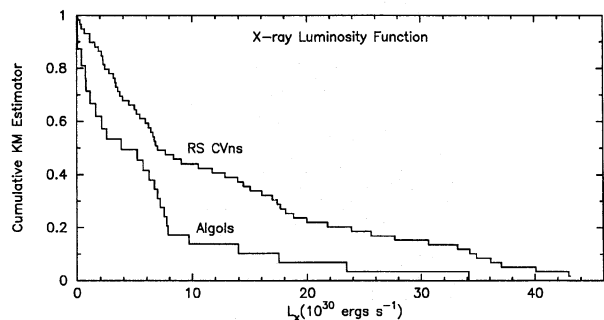


FIG. 2. The cumulative x-ray luminosity function for the RS CVns and Algols based on the Kaplan Meier Estimator.

method to look for the correlations among the following quantities: (a) $\log L_x$ vs $\log \Gamma_2$, (b) $\log L_x$ vs $\log P$, (c) $\log S_x$ vs $\log P$, (d) $\log \Gamma_2$ vs $\log P$, (e) $\log L_x$ vs $\log R$, and (f) $\log \Gamma_2$ vs $\log R$. The results based on the Kendall's τ test and the Buckley–James method are summarized in Table 4. The results from the Spearman's rank order test were consistent with those from the Kendall's τ test and, therefore, are not listed. Below we consider the various correlations individually.

Firstly, the $\log L_x$ vs $\log \Gamma_2$ data shown in Fig. 3 do indeed exhibit a correlation, with a confidence level of 99.5% for the RS CVn binaries. A similar correlation for the Algol types is, however, at best marginal with a confidence level of only $\sim 93.4\%$. The result for the RS CVn binaries appears to be similar to that of Welty & Ramsey (1995), who however did not quantify the correlation. The lines of correlation obtained from the Buckley–James test are shown for the two samples in the Fig. 3. Their slopes are close to unity and not significantly different for the two samples; however, the intercept for the sample of Algols is different from that for the RS CVns resulting in the correlation line being displaced by a factor of ≈ 4 to lower L_x values. A similar plot of the S_x versus Γ_2 (not shown), exhibits a very large scatter, with absolutely no indication of any correlation in the total sample or the individual samples.

Next, we looked at the correlations between $\log L_x$ and $\log P$, and $\log S_x$ and $\log P$ for our two sample. The scatter plots for these variables are shown in Fig. 4(a) and Fig. 4(b), respectively. A marginally significant correlation (Probability=98.86%) is found for the $\log L_x$ vs $\log P$ for the total sample, but no significant correlation is found in either of the two individual samples (see Fig. 4(a)). A significant correlation (Probability $\geq 99.99\%$ for RS CVns and 99.35% for Algols) is, however, found between $\log S_x$ and $\log P$. The lines of correlation are shown in Fig. 4(b). The observed correlation is similar to that reported earlier for the RS CVns by Walter & Bowyer (1981) and Dempsey *et al.* (1993a), and for the Algols by White & Marshall (1983). Data in Figs. 3 and 4(b), both show a general tendency for an Algol binary with a given period to be subluminous by a factor ~ 3 when compared with an RS CVn binary with the

TABLE 4. Results of statistical tests for correlations.

Sample	RS CVn Binaries	Algol-type Binaries	All
(a) $\log L_x$ vs. $\log \Gamma_2$			
Number of Objects	57	29	86
Kendall's τ	0.57	0.458	0.33
Probability ^a	0.0016	0.066	0.021
Intercept ^b	1.15	0.50	0.87
Slope ^c	1.11 ± 0.24	1.04 ± 0.45	0.85 ± 0.23
(b) $\log L_x$ vs. $\log P$			
Number of Objects	59	29	88
Kendall's τ	0.37	-0.034	0.389
Probability ^a	0.036	0.89	0.0067
Intercept ^b	0.59	0.346	0.454
Slope ^c	0.31 ± 0.13	-0.16 ± 0.38	0.33 ± 0.12
(c) $\log S_x$ vs. $\log P$			
Number of Objects	59	29	88
Kendall's τ	-1.17	-0.68	-0.86
Probability ^a	0.0000	0.0065	0.0000
Intercept ^b	0.725	0.08	0.44
Slope ^c	-1.07 ± 0.12	-0.92 ± 0.29	-0.91 ± 0.11
(d) $\log \Gamma_2$ vs. $\log P$			
Number of Objects	57	29	86
Kendall's τ	-0.10	-0.38	-0.25
Probability ^a	0.56	0.106	0.076
Intercept ^b	-0.27	-0.074	-0.21
Slope ^c	-0.05 ± 0.06	-0.40 ± 0.13	-0.12 ± 0.05
(e) $\log L_x$ vs. $\log R$			
Number of Objects	59	29	88
Kendall's τ	0.75	0.41	0.69
Probability ^a	0.0000	0.101	0.0000
Intercept ^b	0.441	-0.023	0.264
Slope ^c	0.70 ± 0.145	0.77 ± 0.52	0.80 ± 0.14
(f) $\log \Gamma_2$ vs. $\log R$			
Number of Objects	57	29	86
Kendall's τ	0.525	0.360	0.421
Probability ^a	0.0039	0.125	0.0024
Intercept ^b	-0.414	-0.35	-0.386
Slope ^c	0.26 ± 0.09	0.27 ± 0.23	0.25 ± 0.08

^a Probability of no correlation

^b For the dependent variable or the y-axis. Based on the Buckley-James Method

^c Based on the Buckley-James Method

same period, consistent with the difference found from the luminosity functions in Fig. 2.

To further examine the reasons for correlation observed between $\log L_x$ and $\log \Gamma_2$ for the RS CVns, we studied the correlations mentioned in the beginning of the section and listed in Table 4. It is found that the RS CVns do indeed show a strong correlation between $\log L_x$ and $\log R$ (probability $> 99.99\%$), and between $\log \Gamma_2$ and $\log R$ (probability 99.15%), whereas the Algols do not show these correlations. Therefore, it seems highly likely that the underlying reason for the correlation observed between $\log L_x$ and $\log \Gamma_2$ in the RS CVns is that both of these quantities are themselves highly correlated with the stellar radii.

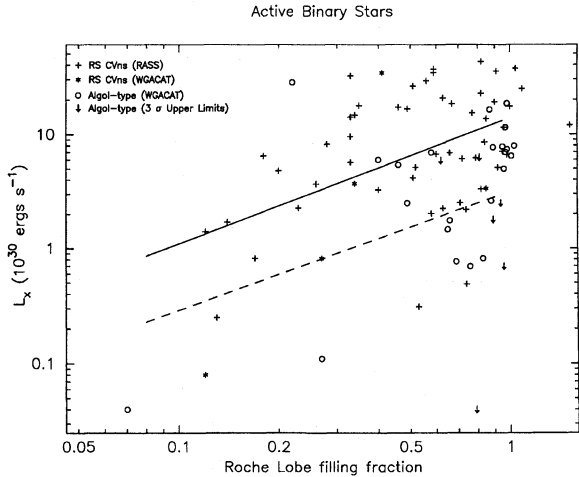


FIG. 3. Scatter plot of L_x against the Roche-lobe filling fraction (Γ_2) for the “active” star in the RS CVns and Algol-type stellar binaries. The lines of correlation from regression analysis have been drawn (solid line is for RS CVns and dashed line is for Algols).

5. DISCUSSION AND CONCLUSIONS

We have studied the x-ray emission properties of 59 RS CVns and 29 “Algols” with well defined orbital parameters and x-ray detections. The x-ray luminosity distributions of the RS CVn-like and the Algol-type stars are quite dissimilar. The Algols are generally subluminescent by a factor $\sim 3-4$ compared to RS CVns with similar orbital periods, confirming the conclusions of White & Marshall (1983) based on a much smaller sample. There is also a lack of Algols with $L_x \geq 10^{31}$ erg s $^{-1}$ compared to the classic and long-period RS CVns in which about 50% of them have such high values. Since the active stars in RS CVns and Algols are believed to be generally very similar, this difference in their x-ray properties is somewhat unexpected. Part of the x-ray deficit of Algols may be due to the fact that they generally contain only one late-type, coronal star, while most RS CVns contain two; however, in RS CVns, one component often will predominate, e.g., provide at least two-thirds of the emission, so that this effect would be expected to produce a much smaller ($\leq 50\%$) difference than the factor of 3 to 4 that is observed. Absorption of x-rays by circumstellar or circumbinary material found to be present in some Algol binaries (Richards 1993) is unlikely to cause such an effect as the large absorption ($N_H > 10^{21}$ cm $^{-2}$) required to suppress the L_x by a factor of ~ 3 is not seen in the soft x-ray spectra of Algols (Singh *et al.* 1995a). White & Marshall (1983) have considered other possible explanations for this difference between the x-ray emission levels of Algols and RS CVns. Their suggestion that, in RS CVns, the x-ray luminosity is enhanced due to energy release from the disconnection/reconnection of magnetic structures that link the two (late-type) components is, we feel, perhaps the most viable one. Detailed MHD modeling of the evolution of interconnecting magnetic loops in such binary systems along the lines suggested by Uchida (1986) and Uchida & Sakurai (1983) is clearly needed to test this hypothesis.

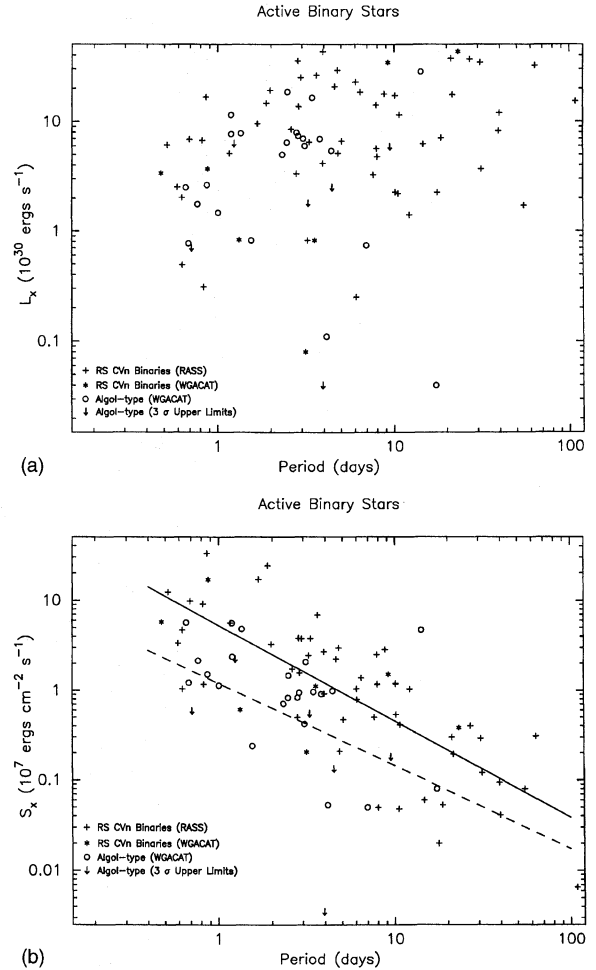


FIG. 4. (a) Scatter plot of L_x against the period of the RS CVns and Algol-type stellar binaries. (b) Same as in (a) for S_x vs the period of the RS CVns and Algol-type stellar binaries. The lines of correlation from regression analysis are as drawn in Fig. 3.

As for the role of mass transfer in enhancing x-ray emission levels, we do not find any convincing evidence for the presence of such an effect in either the RS CVn-like or the Algol-type binaries: as pointed out above, the evidence, in fact, is to the contrary, in that Algol-type binaries are generally subluminescent in x-rays as compared to the RS CVn binaries. This could mean that either the efficiency for the conversion of the mechanical luminosity based on large stream velocities observed by Huenemoerder & Barden (1986) to the x-ray luminosity is very low, or that the conditions for this conversion do not exist in these systems when compared to more compact x-ray binaries. One of the first mechanisms suggested for the generation of x-rays (Harnden *et al.* 1977) is the shock heating of the infalling material either from the Roche lobe overflow or strong stellar winds. The maximum temperature from such a mechanism is ≤ 0.25 keV in the systems under consideration. This is much lower than the temperatures observed in RS CVns and Algols as was first pointed out by White *et al.* (1980) for Algol and subsequently has been shown to be true for a number of RS CVns and Algol-type binaries (Swank *et al.* 1981, Singh *et al.* 1995a).

The major evidence suggesting that there may be a link between mass transfer and x-ray emission in active binaries is the correlation between L_x and Γ_2 for RS CVn systems noted by Welty & Ramsey (1995) that we have also confirmed. However, we regard this as a rather weak argument, because both the x-ray luminosities and the Roche-lobe filling fractions are themselves correlated with the stellar radii in the sample of RS CVn binaries, and thus we regard the correlation of L_x and Γ_2 as merely a by-product of the inherent size dependence of these quantities. Interestingly, there is no obvious correlation of L_x and Γ_2 in the (admittedly smaller) sample of Algol binaries, for which the only correlation that we found was an inverse one between S_x and P , that is nearly identical (in slope) to that found for the RS CVn systems. The fact that the surface x-ray flux appears

highly correlated with the period in both the RS CVns and Algols, suggests that their x-ray activity is more likely related to the tidally induced rotation of these systems enhancing their dynamo activity than to any effects of mass transfer.

We thank the referee for his/her careful reading of the original version of this paper and for finding some miscalculated values in the tables. This research has made use of *ROSAT* archival data obtained through the High Energy Astrophysics Science Archive Research Center, HEASARC Online Service, provided by the NASA-Goddard Space Flight Center; and the SIMBAD database, operated at CDS, Strasbourg, France.

REFERENCES

- Brancewicz, H.K., & Dworak, T.Z. 1980, *Acta Astron.* 30, 501
 Dempsey, R.C., Linsky, J.L., Fleming, T.A., & Schmitt, J.H.M.M. 1993a, *ApJS*, 86, 599
 Dempsey, R.C., Linsky, J.L., Schmitt, J.H.M.M., & Fleming, T.A. 1993b, *ApJ*, 413, 333
 Drake, S.A., Simon, T., & Linsky, J.L. 1989, *ApJS*, 71, 905
 Eggleton, P.P. 1983, *ApJ*, 268, 368
 Giuricin, G., Mardirossian, F., & Mezzetti, M. 1983, *ApJS*, 52, 35
 Hall, D.S. 1989, *Space Sci. Rev.* 50, 219
 Hall, D.S. 1976, *IAU Colloquium No. 29*, 287
 Harnden, Jr., F.R., Fabricant, D., Topka, K., Flannery, B.P., Tucker, W.H., & Gorenstein, P. 1977, *ApJ*, 214, 418
 Huenemoerder, D.P., & Barden, S.C. 1986, *AJ*, 91, 583
 Isobe, T., Feigelson, E.D., & Nelson, P.I. 1986, *ApJ*, 306, 490
 Popper, D.M. 1991, *AJ*, 101, 220
 Richards, M.T. 1993, *ApJS*, 86, 255
 Singh, K.P., White, N.E., & Drake, S.A. 1996, *ApJ*, 456, 000
 Singh, K.P., Drake, S.A., & White, N.E. 1995a, *ApJ*, 445, 840
 Singh, K.P., Drake, S.A., & White, N.E. 1995b (in preparation)
- Strassmeier, K.G., Hall, D.S., Fekel, F.C., & Scheck, M. 1993, *A&AS*, 100, 173 (CABS2)
 Swank, J.H., White, N.E., Holt, S.S., & Becker, R.H. 1981, *ApJ*, 246, 208
 Uchida, Y. 1986, *Highlights of Astronomy, Proceedings of the Nineteenth IAU General Assembly, Delhi, India (Reidel, Dordrecht)*, Vol. 7, p. 461
 Uchida, Y., & Sakurai, T. 1983, *Activity in Red-Dwarf Stars, Proceedings of the Seventy-first IAU Colloquium, Catania, Italy (Reidel, Dordrecht)*, p. 629
 Walter, F.M., & Bowyer, S. 1981, *ApJ*, 245, 671
 Welty, A.D., & Ramsey, L.W. 1995, *AJ*, 109, 2187
 Welty, A.D., Hall, J.C., Patterer, R.J., & Ramsey, L.W. 1992, in *7th Cambridge Workshop on Cool Stars, Stellar Systems, and the Sun*, edited by M. Giampapa and J.A. Bookbinder, *ASP Conf. Ser. 26 (ASP, San Francisco)*, p. 116
 White, N.E., Giommi, P., & Angellini, L. 1994, *IAUC*, 6100
 White, N. E., & Marshall, F.E. 1983, *ApJ*, 268, L117
 White, N. E., Holt, S.S., Becker, R.H., Boldt, E.A., & Serlemitsos, P.J. 1980, *ApJ*, 239, L69

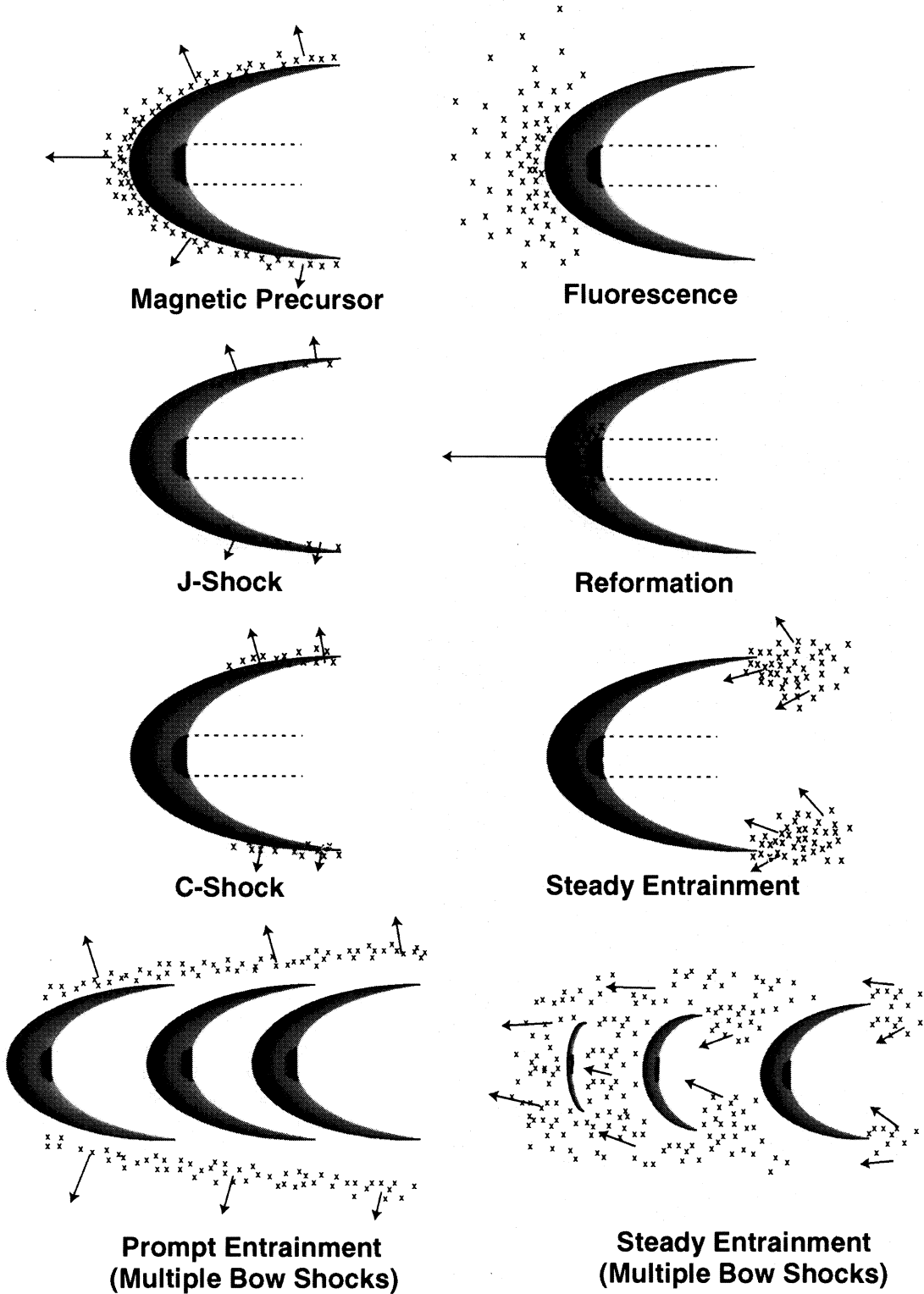


FIG. 4. The relationship of H₂ emission (X's) to bow shocks in stellar jets expected for various models. The shaded areas show regions of optical line emission that arise in the hot gas behind J shocks in the bow shock and the Mach disk. Arrows denote the velocity of the H₂ with respect to the ambient medium. The jet flows from right to left between the dotted lines in each example.

Hartigan *et al.* (see page 2470)